

# CFD-based Optimization of Scroll Compressor Design and Uncertainty Quantification of the Performance Under Geometrical Variations

Cavazzini G.<sup>1</sup>, Giacomel F.<sup>1</sup>, Ardizzon G.<sup>1</sup>, Casari N.<sup>2</sup>, Fadiga E.<sup>2</sup>, Pinelli M.<sup>2</sup>, Suman A.<sup>2</sup>, Montomoli F.<sup>3</sup>,

<sup>1</sup> Department of Industrial Engineering, University of Padova

<sup>2</sup> Department of Engineering, University of Ferrara

<sup>3</sup> Department of Aeronautics, Imperial College London

## Abstract

Positive displacement (PD) machines are widely used in several applications such as in vapor and power generation systems. Nevertheless, their design is still based on standard approaches mainly driven by thermodynamic analysis and theoretical correlations. Geometrical details influence on the machine performance is often neglected. Because of this, PD machines hydraulic efficiency has not really been improved.

The present work shows an innovative design strategy aimed at maximizing the machine efficiency by topology optimization. The geometry of a scroll compressor has been parametrized. The parameters were optimized with a Particle Swarm Optimization (PSO) based procedure integrated with Computational Fluid Dynamics (CFD) to achieve the maximum efficiency. In order to better understand the influence of these parameters on machine performances, a Design of Experiment (DOE) approach was also used. Afterwards an Uncertainty Quantification framework is applied to the compressor to identify the reliability of the optimal design subject to geometrical variations. Among all the investigated parameters, the most important seem to be the high-pressure port shape and size. Performance are highly affected also by the number of coils which defines the built-in compression ratio.

## 1. Introduction

Positive displacement (PD) machines have a wide range of applications in modern engineering problems. Specifically, such machines have been used as either compressor or expander in vapor compression and power generation systems (e.g. Organic Rankine Cycles, ORCs).

Among the several type of PD machines available, scroll-type expanders/compressors are receiving more and more attention from researchers. This type of machine is highly appreciated for its large operational range, reliability, compact structure, low number of moving parts and low level of noise and vibrations [1]. In particular, the vast majority of applications of ORCs with power output lower than 10-20 kWe are equipped with a scroll as expander. Examples of such applications can be found in [2] [3] [4] [5] [6].

The advantages of scrolls are remarkable even when operated as compressors. Several refrigeration systems and heat pumps are indeed equipped with scroll compressors, such as [7] [8]. In [8] the scroll is used to process CO<sub>2</sub>. This represents a further possible application of the scroll-type configuration, making such machine particularly attractive.

Nevertheless, their design is still based on standard approaches mainly driven by thermodynamic analysis and theoretical correlations aimed at defining the resulting shape from the volumes to displace. No attention has been ever paid to the geometrical details in order to verify their influence on the machine performance. Because of this, their efficiency has not been improved in the years and, in more than one case, its poor value

negatively affects the global efficiency of the system in which they are applied. This is true not only for scrolls but for positive displacement machine in general, as highlighted by Ziviani et al. [9] clearly stating that the low efficiency values of PD machines represent the “bottleneck to raise the ORC system efficiency” and identified the main cause of this low efficiency in the modeling difficulty.

In particular, the design of the scroll is typically driven by the thermodynamic analysis and the evolution of the chamber volumes is therefore retrieved [10]. The outcome of such procedure defines by geometrical modelling (such as [11]) uniquely the shape of the spirals. The design of the machine, on the other hand, can be optimized and there are other parameters that are not strictly derived from this procedure (such as the high-pressure port shape). Therefore, there is some room for improvement in the definition of the best solution, and an optimization procedure can be set-up.

Some attempts to improve the scroll design have been presented in literature and one of the most interesting was proposed by Bell et al. [12]. In their work they developed an analytical model to evaluate the thermodynamic irreversibility sources in the operation of a scroll compressor. By applying this model to a starting geometry, the authors were able to identify three main losses. Then, in three steps – one for each loss source - after some parameter assumptions and mathematical simplifications, they were able to analytically determine optimal values for few geometrical parameters. Even though some improvements in efficiency was achieved, the need of assumptions and simplifications, required by the analytical approach, limited the achievement of a global design optimization. To the authors knowledge, nobody used Computational Fluid Dynamics (CFD) to evaluate the performance in the design phase so far and nobody ever proposed an optimization procedure of the scroll design integrating the CFD within the design process. Although some examples of CFD-based design procedure can be found in literature [13], [14], [15], all of them are related to turbomachines, whose complex design has favored the development of dedicated CFD approaches from decades. Regarding scroll machines, over the last years, researchers have started to analyze their performance using numerical approaches. The growing computational power available has made Computational Fluid Dynamics (CFD) a viable way to investigate the flow behavior inside this class of machines. The computational cost until few years ago was limited by the number of time steps required to model the unsteady behavior of a PD machine. Moreover, there are some big challenges associated to the numerical investigation, such as the grid deformation and the modelling of real gas equations in case of refrigerants [16]. Several numerical techniques have been developed over the years for tackling the mesh motion problems (e.g. dynamic mesh, remeshing, overset/immersed boundaries methods), and a review of their performance and limitations when applied to PD machines is shown by [17].

In this analysis, a CFD-based design optimization is carried out. First, the equidistant curves approach [11] was applied to properly parametrize a scroll geometry. This approach identified a finite number of input geometrical parameters whose definition allowed to obtain the scroll geometry. Then, a proper CFD approach was defined to numerically analyze the scroll efficiency. Then, an optimization design procedure aimed at maximizing the scroll efficiency was developed by integrating the parametrization model with the CFD approach and an optimization algorithm. Meta-heuristic optimization algorithms are generally chosen in design optimization problems because of their fast-convergence performance [18].

Among the available meta-heuristics optimization algorithms, the authors have decided to adopt the in-house developed Particle Swarm Optimization (PSO) algorithm (ASD-PSO) [19]. This choice was driven not only by its optimal convergence performance, but also by the possibility of customization to the specific design procedure, both allowing to speed up the optimization process. Then, an uncertainty quantification of the achieved performance under geometrical variations was carried out. To reduce the computational efforts, once identified the most influencing design parameters by means of the optimization procedure results, a DOE approach with lattice sampling scheme was applied.

## 2. Geometry and Parameters Definition

The optimization procedure carried out in this work aims to find the best sets of parameters that can maximize the efficiency of the scroll compressor given specific boundary conditions. In order to do so, a baseline geometry is required to develop a geometry generator that can handle all the parameters from both the peripheral and, more important, the central profiles of the scrolls.

The type of profile used in this work is the Perfect Meshing Profiles (PMP). The simpler circle involute profiles cannot match perfectly, resulting in larger clearance in the central portion of the scroll compressor and smaller built-in volume ratio.

There are different approaches to modify the central profile of a scroll and wrap it into a PMP. The approach used in this work is the equidistant curve approach from [11]. This method utilizes the equations for the scroll wraps central midline, defining the two wraps as simple offset. The advantage of this formulation relies on the reduced number of equations involved and the simple management of relative positions of the two wraps, allowing more precise CFD settings and control over the flank gaps. The application of the algorithm here presented to a such a basic geometry should be considered as a demonstration of the generality of the procedure and of the results.

The scroll midline is made of a circular involute and a circular arc.

The equations for these two entities are as follows:

$$\begin{cases} x_{arc}\theta = x_c + R_m \cos \theta \\ y_{arc}\theta = y_c + R_m \sin \theta \end{cases} \quad \text{for } \theta \in [\gamma + \pi, \gamma + \pi + \lambda]$$

Equation 1 Coordinates for circular arc points

$$\begin{cases} x_{inv}\theta = R_b \cos \theta + R_b \left( \theta + \frac{\pi}{2} \right) \sin \theta \\ y_{inv}\theta = R_b \sin \theta - R_b \left( \theta + \frac{\pi}{2} \right) \cos \theta \end{cases} \quad \text{for } \theta \in [\phi, \phi_{end}]$$

Equation 2 Coordinates for circular involute points

Where  $x_c$ ,  $y_c$  and  $R_m$  are the coordinates of the center of the circular arc and the radius of the circular arc at the midline;  $\gamma$  is the modified angle (angle between the center of the arc and the x axis);  $\lambda$  is the central angle of the circular arc;  $R_b$  is the radius of the involute generating circle;  $\phi$  and  $\phi_{end}$  are the starting and ending angle of the involute.

The two scroll profiles are then obtained by offsetting the midline in both directions by half of the orbit radius  $R_b$ . The resulting geometry is shown in Figure 1

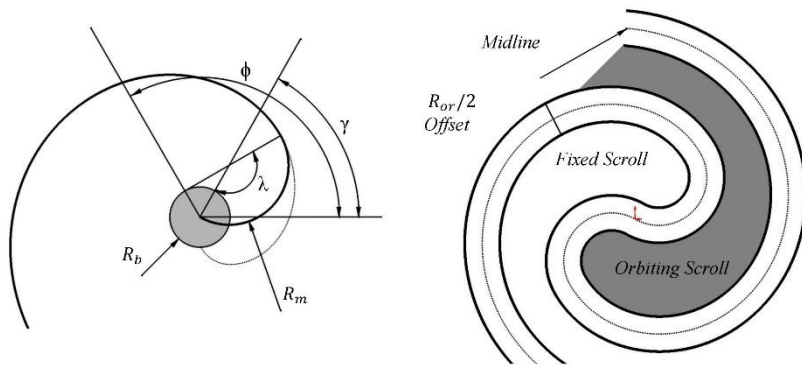


Figure 1 PMP midline angles and parameters

The following design parameters were taken into consideration for the optimization procedure.

From this set of parameters all the angles and radii in Equation 1 and Equation 2 can be easily calculated.

- Orbit radius
- Thickness of the scroll wraps
- Involute starting angle (where the circular arc ends)
- Involute ending angle (defines the number of coils)
- Height of the scroll walls
- Radius of the central port

Orbit radius and thickness define the pitch of the coils. The pitch eventually defines the shapes of the chambers, which are the isolated volumes between fixed and moving scroll, in which the air is displaced and compressed from inlet to outlet. Scroll thickness affects mainly the chamber length, the orbit radius affects both length and maximum width of the chambers. However, the built-in compression ratio largely depends on the number of wraps.

These parameters were optimized with the PSO algorithm [19]. The radius of the central port does not change the shape of the wraps, but it has been proven to be a fundamental parameter in the optimization procedure. The port radius has the physical constraint to be smaller, than the last chamber of the scroll. The dimensions of this chamber are dependent on other parameters such as the orbit radius. In the optimization procedure the radius of the central port was expressed in a dimensional value related to its maximum size, which was the maximum width of the last chambers.

### 3. CFD Approach

As already mentioned in the introduction section, numerical CFD simulation of Positive Displacement machine are extremely complex.

The optimization proposed in this work is based on full three-dimensional CFD analyses of the scroll compressor. The simulation of such a machine, and generally speaking of PD machines, is not straightforward as there are some intrinsic features of the operation that add extra costs to the simulations and require dedicated tools. The variation of the working chamber geometry, the presence of different length scales and the intrinsic transient behavior of the flow are some of the challenges related to these investigations. Additionally, these simulations must be included in an automated workflow, as the optimization procedure requires multiple runs to properly describe the response surface.

In light of these considerations, the software chosen to be integrated in the current procedure is Pumplinx-v.4.6. This CFD solver proved to be robust and accurate in simulating scroll compressors [6], [20]. The operation of the machine is replicated by means of the deformation of a structured grid, that allows for high distortion levels without disrupting its quality [21]. The initial mesh is indeed stretched by the motion of the spiral, but the high orthogonality levels and its topology definition make it possible to use the same connectivity without remeshing requirements in the working chamber and the gaps. In this work, the grid parameters are chosen after a sensitivity analysis and are kept fixed for all the simulations. Due to the variation in the geometry, the number of elements changes in the various simulation, but the overall number is always above 200,000 elements. The spiral area is meshed with the structured grid above described. The ports, on the other hand, are discretized by means of a trimmed, hex-dominated mesh, that communicates with the structured mesh via non-conformal interfaces. The simulations run fully turbulent, with  $k - \epsilon$  turbulence model.

In order to assess the accuracy of the CFD simulation, a test case where some experimental data were available, has been used [11]. The geometry parameters as well as the operating conditions for the simulation are taken from [11]. In particular, the two scroll wraps are generated with height  $h=40$  mm, thickness  $\delta=4.5$  mm, orbit radius  $R_o=5.5$ . After the two wraps are drawn, the orbiting scroll is translated by

5.47 mm. This distance is smaller than the orbit radius thus it leaves a flank gap of  $30 \mu\text{m}$ . The discharge port is situated at the scroll center, tangential to the fixed scroll at the final meshing point. Operating condition are  $p_{in}=1$  bar,  $p_{out}=7$  bar,  $T_{in}=293$  K,  $\omega=3000$  rpm. The results of the test showed values close to the experimental ones from [11]. The mass flow rate from the simulation was  $m_{air}=0.0108$  kg/s, thus the model and the simulation method are verified.

The optimization procedure was then carried out starting from this first configuration and set of boundary conditions. The simulations run fully turbulent, with two equations  $k - \epsilon$  turbulence closure.

## 4. Optimization Procedure

The optimization procedure for maximizing the scroll efficiency, is carried by adopting the ASD-PSO (Adaptive Search Domain – PSO) [19], a recent evolution of the standard PSO already successfully adopted in other optimization problems [18]. Based on a metaheuristic approach, the ASD-PSO algorithm searches for the optimal values of the independent variables, namely the input geometrical parameters previously mentioned, in order to achieve the maximum efficiency (objective function).

The optimization procedure ends when the optimization algorithm reaches the maximum efficiency and it is not able to find a different solution (i.e. different values of the input geometrical variables) for further increasing the objective function value.

The optimization is carried out automatically leveraging the scripting potential of Matlab and it involves several steps, calling different software. First, the procedure is initialized by assigning starting values to the input geometrical parameters (see Section 3). Then, the geometry is defined in Matlab, by applying the parametrization model described in the previous section, and the three-dimensional model is built in Solid Works. Afterward the CFD software, namely Pumplinx, numerically analyses the proposed geometry and determines the value of the objective function. Then, the optimization algorithm decides new values for the input geometrical parameters and the iteration starts again

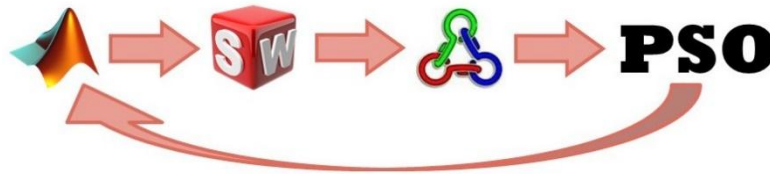


Figure 2 Optimization Procedure

All the different softwares are executed with batch commands using Matlab. A script that runs the whole procedure uses other scripts or executable files to run each of the steps. The steps of the procedure are the following.

- A Matlab script draws the two splines for the orbiting and fixed scrolls using the previously discussed equations. Then it writes two text files containing the coordinates of all the points of the splines. The same script uses the inputs and the boundary conditions to write the case file for the CFD simulation.
- In the next step the splines are built in Solidworks starting from the points of the text files and extruded. This operation creates a set of surfaces that are compatible with the solver template for scroll compressors. These surfaces are then exported into STL files. All of these operations are carried out using Solidworks macros.
- The case file written in the first step is executed. Simerics Pumplinx is used as solver with batch command. Pumplinx imports the STL files and creates the fluid domain with its template meshing



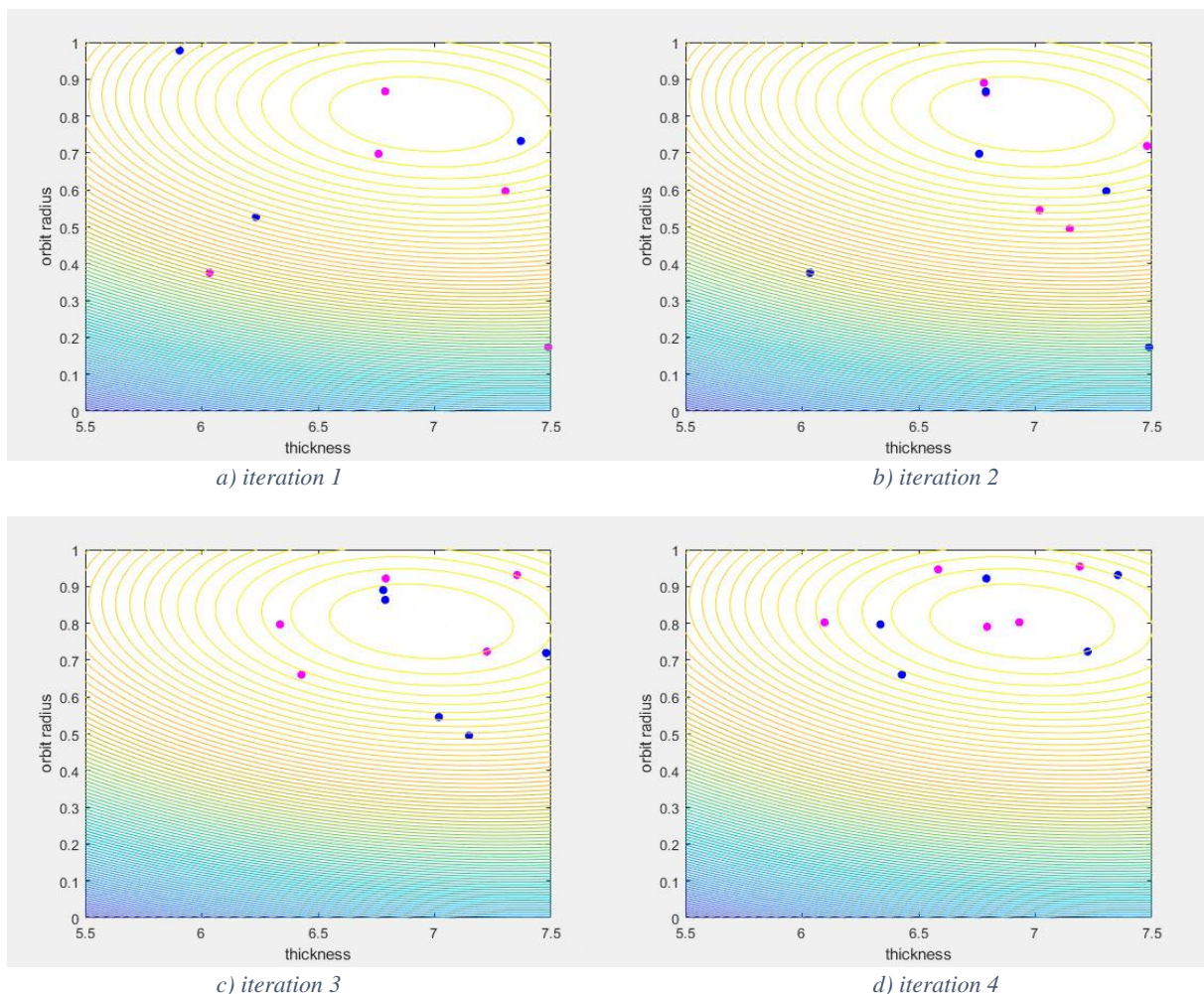
1 tool. Input and output pipes are created as well as all the interfaces. Then the calculation is  
2 performed. Results are exported as text files

- 3 • Another Matlab scripts reads the result files. In particular the difference of mass flow between inlet  
4 and outlet is checked to be within a defined range of tolerance. This is to check whether the  
5 calculation has converged or not and, if so, the efficiency is calculated and saved in a report file.
- 6 • Eventually the PSO collects the results for the performances of a fixed amount of geometries: if the  
7 swarm is set to be of 5 particles, 5 different geometries are tested and for each one the efficiency is  
8 calculated. The PSO algorithm, given the efficiency, generates 5 new sets of parameters, with the  
9 aim to select the parameters that give higher efficiency. Then the procedure starts over.

## 14 5. Results

16 Since CFD-based design optimization procedure are extremely CPU- and time-consuming, the general  
17 practice is to limit the parameters to optimize to those really affecting the results of the objective function,  
18 namely the scroll efficiency.

20 To understand the metaheuristic principle of the algorithm, Figure 3 Evolution of the swarm particles over  
21 the resulting response surface in four different iterations of the optimization process. Blue dots: positions of  
22 the swarm particles at the beginning of the iteration; pink dots: positions for next iteration reports four  
23 different instants of an optimization process, highlighting the swarm movements towards the optimum  
24 solution. The contour in the background is the response surface of the optimization, given by a interpolation  
25 of efficiency results achieved by all the geometrical configurations analyzed during the searching process.



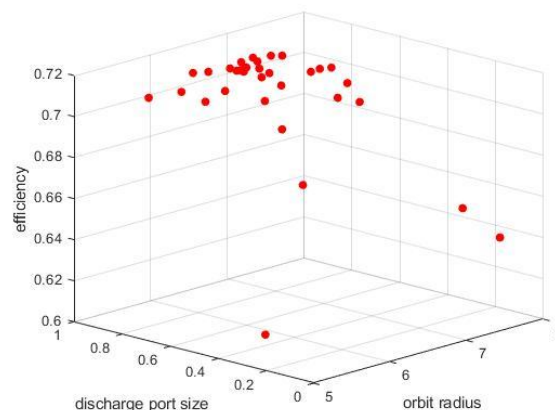
1  
2 *Figure 3 Evolution of the swarm particles over the resulting response surface in four different iterations of the optimization process.*  
3 *Blue dots: positions of the swarm particles at the beginning of the iteration; pink dots: positions for next iteration*

4 Each dot represents a particle of the swarm, which is a possible solution to the optimization problem,  
5 characterized by a combination of values of the three optimization variables. The blue dots represent the  
6 swarm particle positions at the beginning of the iteration  $i_{th}$  and the pink dots their positions at the end of the  
7 same iteration. The pink dots of iteration  $i_{th}$  become the blue dots in iteration  $i_{th+1}$  and so on. Iteration after  
8 iteration, the swarm investigates (in a metaheuristic way) the search domain and upgrades the geometrical  
9 solutions, clearly moving towards the region of maximum efficiency. However, each investigated solution  
10 requires a CFD simulation to determine the resulting efficiency and the more the variables to optimize the  
11 more the solutions to investigate and hence the CFD simulations to carry out.

12 So, to avoid unnecessary huge computational efforts, the mutual interactions between input geometry  
13 parameters and their degree of influence on the scroll efficiency was first investigated by carrying out  
14 optimization procedures considering only two or three design parameters as optimization variables per time  
15 while the rest of them was kept constant.

16 At the beginning all the calculations were conducted keeping the number of revolutions per minute constant  
17 as well as the pressure values at inlet and outlet. Having these values fixed makes it simpler to set the initial  
18 boundary condition and to run the first batch of simulations. These showed which parameters had more  
19 influence on the efficiency and how the mass flow would change with the geometry. This had two purposes:

- 20 1. by varying only the most valuable parameters, two at a time, we could limit the computational effort  
21 and visualize the results with response surfaces, plotting the efficiency as function of parameter 1  
22 and parameter 2. This allows to appreciate the degree of influence of the different parameters on the  
23 objective function. For example, in Figure 3 Evolution of the swarm particles over the resulting  
24 response surface in four different iterations of the optimization process. Blue dots: positions of the  
25 swarm particles at the beginning of the iteration; pink dots: positions for next iteration, it is clear that  
26 the orbit radius (values on the y axis) influences the efficiency more than the thickness (x axis).  
27
- 28 2. the mass flow rate can be calculated as function of the two parameters as well. Knowing this  
29 function, adjustment can be made in the angular velocity or in the number of scroll wraps in order to  
30 keep the mass flow at a constant value.  
31  
32  
33  
34  
35  
36  
37  
38  
39



40  
41  
42  
43  
44  
45  
46  
47  
48  
49  
50  
51  
52  
53 *Figure 4 PSO optimization results*

54 Figure 4 shows the results of a 2-parameter optimization procedure in a 3D response surface. Each dot  
55 represents the positions of the swarm particles during the searching process, showing all the history of the  
56 procedure. The swarm moves towards the most promising search area characterized by solutions showing  
57  
58  
59  
60  
61  
62  
63  
64  
65

higher efficiency values and the concentration of tested geometries increases around the best found solution so far, highlighting the refinement scope of the algorithm.

The analysis of the obtained response surfaces by the design optimization procedures allowed to identify the most influencing parameters: orbit radius and discharge port size

Once established the parameters to consider and verified the regular unimodal shape of the response surface, it was convenient to switch the approach from the PSO algorithm to a DOE approach with lattice sampling scheme. With a lattice scheme, equally spaced sampling points are selected within the domain, given by the lower and upper bounds of the investigated parameters. In case of a reduced number of optimization variable, this approach allows to obtain the same response surface function with less but better spaced points. This reduces the number of simulations needed for the drawing of a response surface and consequently the calculation time in comparison with a PSO-based optimization procedure.

So, only the two most influencing parameters (orbit radius and discharge port size) were simultaneously considered: for each parameter, four fixed values were chosen within the domain, which is the same as the one used for the PSO calculations (see Figure 4). The resulting 16 combinations of the two parameters values defined 16 possible geometries of the scroll compressor, summarized in Table 1.

Table 1 Lattice sampling results

| ID | Orbit Radius [mm] | Discharge port size [-] | ID | Orbit Radius [mm] | Discharge port size [-] |
|----|-------------------|-------------------------|----|-------------------|-------------------------|
| 1  | 5.0               | 0.3                     | 9  | 5.0               | 0.7                     |
| 2  | 6.0               | 0.3                     | 10 | 6.0               | 0.7                     |
| 3  | 7.0               | 0.3                     | 11 | 7.0               | 0.7                     |
| 4  | 8.0               | 0.3                     | 12 | 8.0               | 0.7                     |
| 5  | 5.0               | 0.5                     | 13 | 5.0               | 0.9                     |
| 6  | 6.0               | 0.5                     | 14 | 6.0               | 0.9                     |
| 7  | 7.0               | 0.5                     | 15 | 7.0               | 0.9                     |
| 8  | 8.0               | 0.5                     | 16 | 8.0               | 0.9                     |

For all the scroll geometries of Table 1, efficiency values were computed and then fitted by adopting the same interpolation method used for the PSO results (Figure 5).

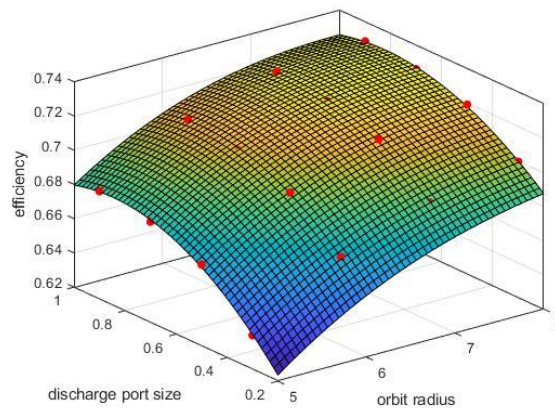


Figure 5 Response surface obtained by lattice sampling approach: efficiency vs. discharge port size and orbit radius. the red dots are the results for the equally spaced sampling points

The results confirmed the similar trend and values of the response surface obtained by lattice (Figure 5) in comparison with that obtained by PSO (Figure 4).



Once verified the effectiveness of the time-saving lattice sampling approach in investigating the parameters dependency, a second step of optimization procedures was carried out considering the user requirements as design constraints, namely constant values of mass flow rate and pressures at scroll inlet and outlet.

However, in positive displacement machines the mass flow rate is related to the rotation speed of the machine and to the geometry, namely to the total volume displacement in one revolution. In particular, in the scroll geometry model here proposed, the total volume displacement in one revolution is related to the orbit radius, affecting the scroll size, and to the number of wraps, affecting the number of volumes discharged by the scroll in one revolution. So, to fulfill the constraint of a constant value of the mass flow rate (around 0.11 kg/s), in the CFD simulations, two different approaches can be adopted:

- i. To fix the number of wraps to 4 full wraps. This means that the midline generating spiral has a involute ending angle  $\phi_{end}$  equal to 4 times  $2\pi$ . The actual number of physical wraps is smaller due to the center geometry correction.

In this case, depending on the radius orbit, a different value of total volume is displaced by the scroll, and the rotation speed of the scroll was then determined consequently. The scroll with smaller orbit radius is rotating at higher speed (3000 rpm) to compensate the low value of total volume per round discharged by the scroll, while for larger geometries the angular velocity is lower.

- ii. To fix the scroll rotation rate to 3000 rpm. In this case, the mass flow rate was kept constant by lowering the number of wraps and keeping the volume of the first chamber fixed. Geometries with smaller orbit radius have higher number of wraps. This means that the scroll geometries with higher orbit radius have less wraps and consequently a smaller built-in volume ratio.

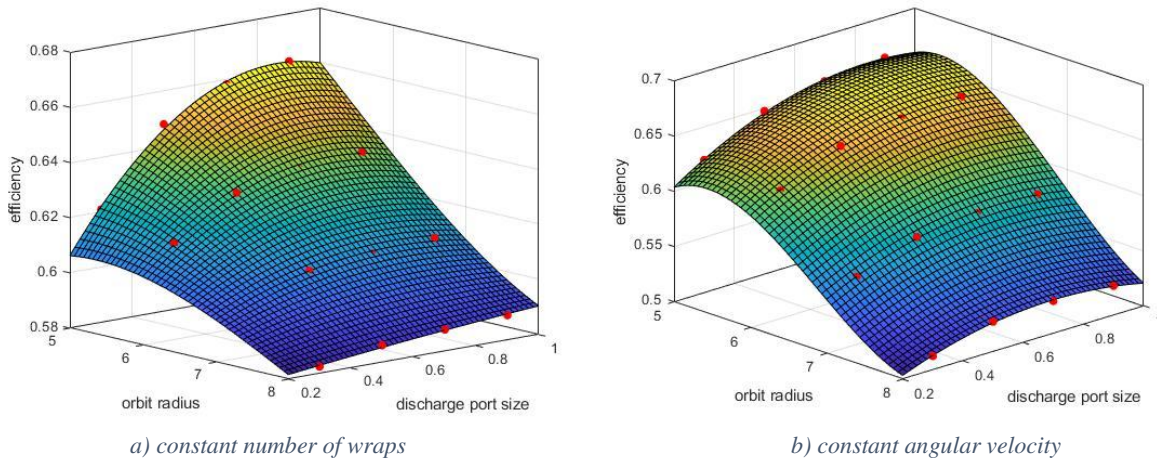


Figure 6 Scroll efficiency vs. orbit radius and discharge port size. Response surfaces for two design approaches: constant number of wraps with variable rotation rate; constant angular velocity with variable number of wraps

Figure 6 shows the response surfaces in terms of efficiency as function of orbit radius and discharge port size for the two different approaches. The size of the discharge port doesn't affect the mass flow rate.

Both the surfaces in Figure 6 show that efficiency has its best value with larger discharge port, even if this can reduce the built-in volume ratio. A larger discharge port creates some clearance connecting one of the two last chambers to the outflow before the other chamber. This fact however does not seem to affect the efficiency compared to the reduction of the local fluid dynamic losses by reduction of the outlet fluid velocity. In both cases it is also clear that smaller orbit radii give higher efficiency, but the optimal value depends on the design approach (fixed wraps or fixed rotation rate) whose choice is mainly driven by technical and/or economical constraints, such as size limits or motor characteristics (synchronous or asynchronous, with or without inverter, etc...).

In particular, with the “fixed number of wraps” approach (Figure 6a), the shape of the response surface shows two interesting results. First, the orbit radius has less influence on the performance than the discharge port size. Second, there is not a global best efficiency point, suggesting that, with this approach, a smaller orbit radius operating at higher speed might achieve even higher value of efficiency. The surface also shows how with smaller machines the discharge port size has greater impact on the efficiency. With smaller machines, the constraint on the mass flow (which is generally a design requirement) forces the designer to adopt higher rotational speed, implying higher fluid velocity at the discharge. Since fluid dynamic losses are directly proportional to the square of the fluid velocity, it is necessary to increase the discharge port size in order to avoid a significant drop of the scroll efficiency.

With the “fixed rotation speed” approach (Figure 6b), we can see a more marked decrease in efficiency with increasing values of the orbit radius. The reason of this results is related to the needs of keeping the volume of the first chamber constant while reducing the number of wraps for compensating the increasing in size. This makes the machine work in heavy under-compression conditions at the design operating point, introducing losses and lowering the efficiency.

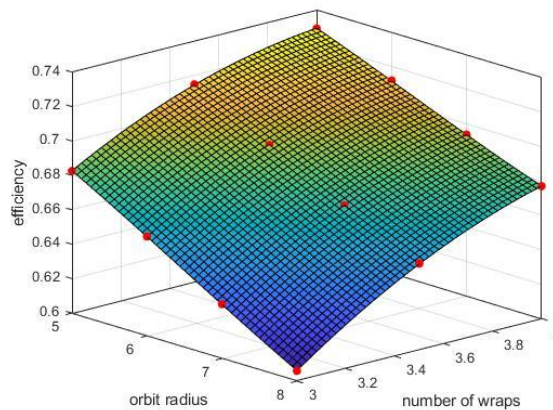


Figure 7 Scroll efficiency vs. orbit radius and number of wraps: response surface at constant discharge port size.

The influence of the under-compression operating condition on the machine performance can be also seen by varying the number of wraps in the “variable rotation rate” approach. Figure 7 reports the efficiency values achieved by scroll geometries, being the discharge port size and mass flow rate constant. Being the mass flow rate fixed, geometries with small orbit radius and high number of wraps are expected to operate at similar rotation rate than geometries with high orbit radius and small number of wraps.

Table 2 Number of wraps and corresponding built-in compression ratio. Variations in the orbit radius don't affect the compression ratio.

| <i>N.of Wraps</i> | <i>Built-in Comp Ratio</i> |
|-------------------|----------------------------|
| 3                 | 3.65                       |
| 3.5               | 4.47                       |
| 4                 | 5.29                       |
| 4.5               | 6.11                       |

So, in terms of fluid dynamic losses no significant differences are expected. However, Figure 7 highlights a significant drop of scroll efficiency for the geometries with higher orbit radius and smaller number of wraps. The reason is that for these configurations the smaller number of wraps reduces the built-in volume ratio and makes the machine operating in under-compression conditions, causing a decrease in efficiency. Table 2 show the correlation between the-built in compression ratio and the number of wraps, while thickness and orbit radius are not significantly affecting the compression ratio.

A positive influence of an increase in the thickness of the scroll wraps was highlighted in Figure 8. Given a fixed value of orbit radius with fixed number of wraps, the increase of the thickness brings slightly better performances. Thickness and orbit radius are both defining the chambers shape. Higher values of thickness make longer chambers a given orbit radius. On the other hand, with fixed thickness, higher values of orbit radius result in both longer and also wider chambers. All these aspects, together with a varying rotation rate, can affect turbulence, ventilation losses, flank gap leakages and the flow field in general, thus many aspects are involved in the response surface shown in Figure 8.

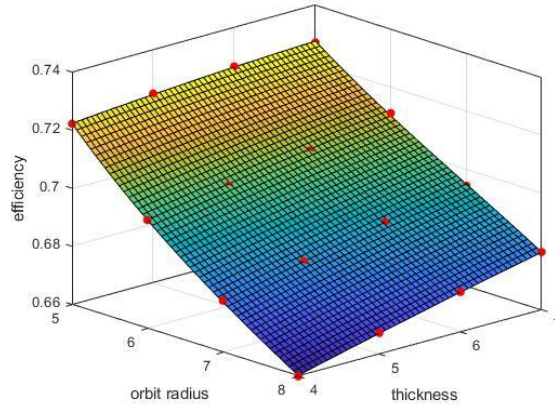
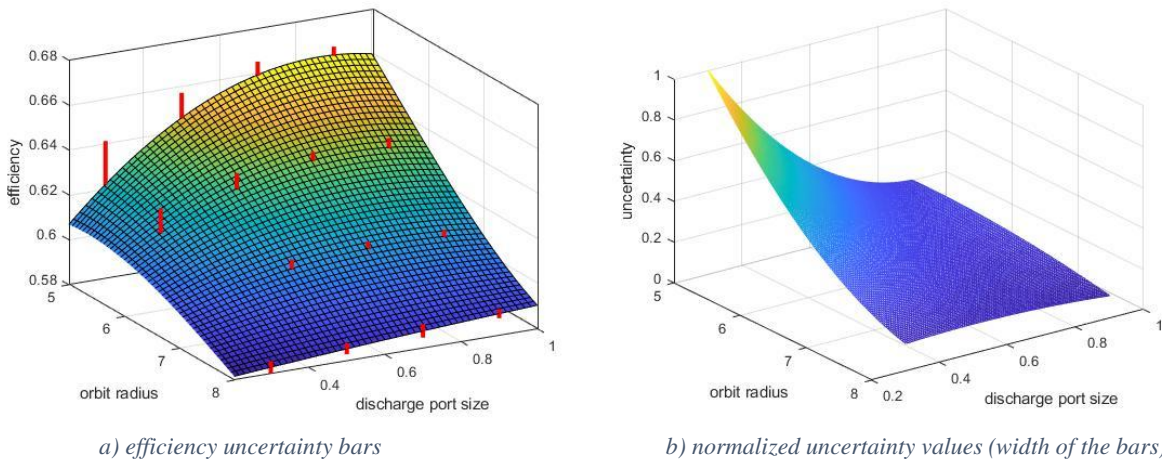


Figure 8 Efficiency vs. orbit radius and thickness of the scroll wraps: response surface for constant mass flow rate and constant number of wraps

## 6. Uncertainties Quantification Analysis



a) efficiency uncertainty bars

b) normalized uncertainty values (width of the bars)

Figure 9 Monte Carlo Method: uncertainties with 6 sigma confidence, constant number of wraps, same geometries and conditions as Figure 6a

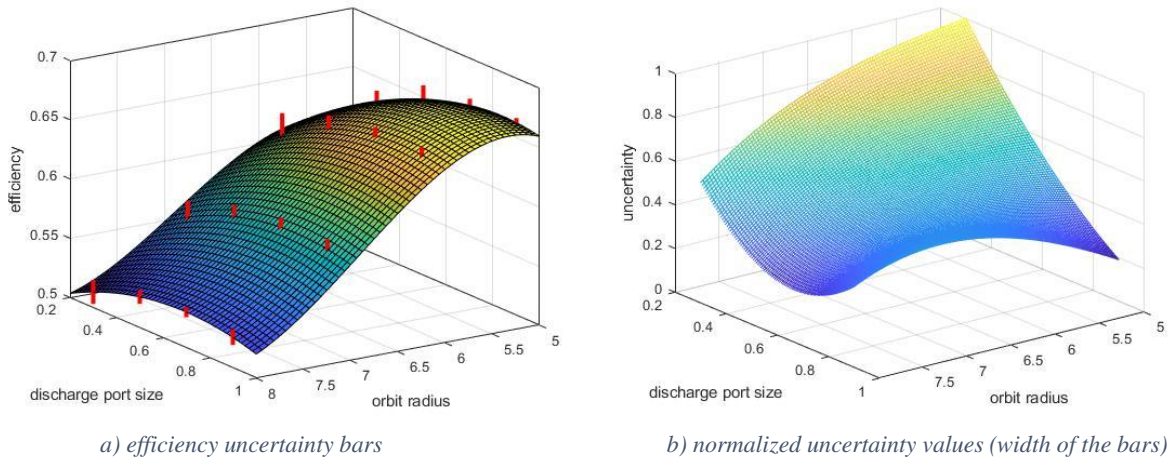


Figure 10 Monte Carlo Method: uncertainties with 6 sigma confidence, constant number of wraps, same geometries and conditions as Figure 6b

Due to the smoothness of the response surface from the input parameters, a lattice sampling method is used to build a series of response surfaces. As described in section 5, these surfaces, have a rather extended efficiency plateau in the nearby of the Best Efficiency Point (BEP). This is particularly clear, for example, from Figure 6. By using a Monte Carlo method and the response surface is possible to quantify the relative importance of geometrical variations on the scroll performance.

The machine under investigation, as all positive displacement machines, is characterized in its performance by the gap size and, generally speaking, by the manufacturing procedure. It is therefore of interest to understand the impact small variations have on the performance. This might lead to different considerations with respect to the surrogate curve that has been described in the earlier paragraphs. To this scope, a robust analysis has been carried out. The objective of this step is to understand the extent to which different designs (found by the optimization) are sensitive towards manufacturing variations.

The analysis has been carried out thanks to a Monte Carlo approach. Monte Carlo simulations are a widely used approach to tackle robust design analyses of chemical processes [22], control systems [23] and industrial products [24]. The same procedure is applied here, sampling the response surface in order to keep the computational effort of the method low. The parameters that have been used for such investigation are relative to the typical geometry variations that are expected for the machining procedure of the scroll. Therefore, a standard deviation of 20 micron and 100 samples per result point were used. Figure 9 and Figure 10 show the uncertainty bars and values referred to the two response surfaces in Figure 6 obtained with the Monte Carlo Method.

These show the tolerance on the efficiency with confidence of  $6\sigma$ . Around the best efficiency point the uncertainty values are lower than other areas where a small modification of geometry can cause a wide impact on efficiency.

By testing the optimized surface with the current procedure, a non-uniform impact of the analyzed parameters on the performance has been detected. Specifically, the areas that are affected the most by a slight variation of the design parameter are the ones that are characterized by the lowest efficiency.

On the other side, small variations of the scroll performance due to variation of the design parameters characterize the geometries around the BEP and hence the optimal design strategy identified in the previous section can be considered as robust.



## 7. Discharge Port Shape

The PSO optimization and the response surfaces obtained by DOE approach suggested that one of the most important parameters driving the scroll performance is the discharge port size and the optimal design strategy suggests the adoption of large discharge port since the benefits related to the reduction of the fluid-dynamic losses resulted to be greater than the possible negative impact of the decrease in built-in volume ratio due to the clearance connecting one of the two last chambers to the outflow before the other chamber.

However, nowadays the discharge port of scroll machines is circularly or elliptically shaped and only some general results about the location of the port can be found in literature [7].

Since the size of the port resulted to affect the performance, further investigations have been carried out to verify possible benefits deriving from unconventional shape of the port itself.

In particular, since the main drawback of increasing the port size is the onset of clearance reducing the built-in volume ratio, a specific topology of the port has been prescribed, as a bean shaped exit that can follow the shape of the scroll fixed spiral. Two parameters have been introduced to control the space: the length and radius of the inner circle.

Figure 11 reports the efficiency of the scroll as a function of the discharge port area. The same exit area can be achieved with different combinations of inner radius and port length, resulting in different port shape. Figure 11 reports four isolines at constant length (from 10 to 100mm) and two isolines at constant radius (2.5 mm on the left and 7 mm on the right).

The results show that overall a bigger area is insensitive from the port shape. When for manufacturing or integration constraint the area is smaller, it is better to have a port with higher length, that follows the shape of the edge of the scroll (longer bean shape). The variation of the efficiency due to the parameters used for its definition is reported in Figure 11.

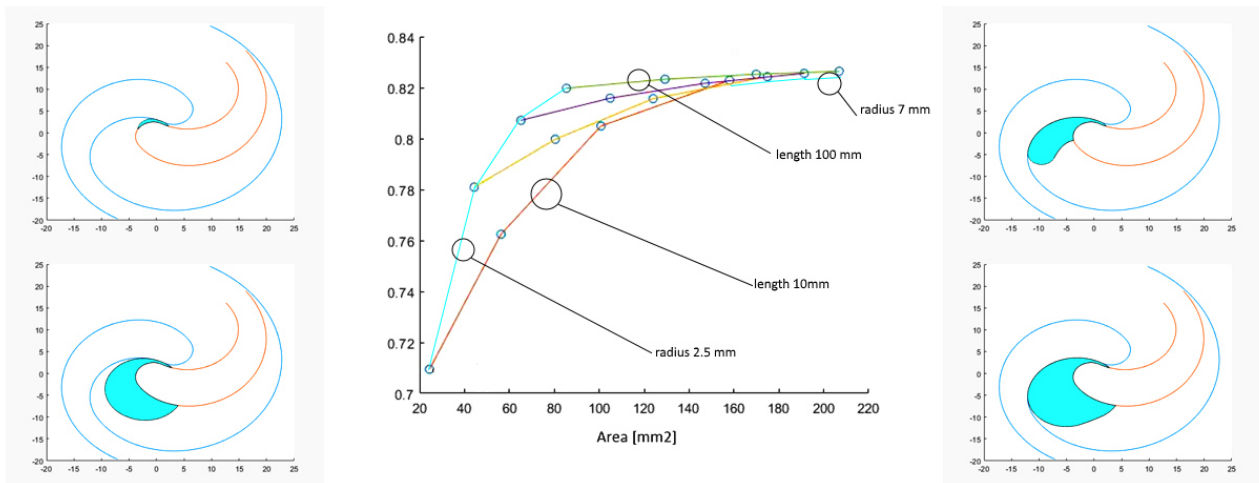


Figure 11 Efficiency vs. discharge port area. Isolines of four constant port lengths (from 10 to 100 mm) and for two constant inner radius (2.5 and 7 mm)

## 8. Conclusions

This work presented a CFD-based innovative design strategy aimed at maximizing the efficiency of a scroll compressor.

The geometry of a scroll compressor has been parametrized and several design parameters, not only related to the main scroll shape but also to geometrical details such as the axial gaps, has been considered in the optimization procedure. A PSO (Particle Swarm Optimization)-based algorithm investigated by



1 Computational Fluid Dynamics (CFD) their influence on the resulting machine performance and optimized  
2 their values to achieve the maximum scroll efficiency.

3 The optimization then continues with Design of Experiment approach, where equally spaced values for the  
4 parameters have been chosen in order to limit the computational effort in the in-depth investigation of the  
5 different design solutions.  
6

7 Out of six (6) parameters investigated only three (3) of them have shown a major impact on the machine  
8 performance: the orbit radius, number of wraps and the discharge port size.  
9

10 In particular, small orbit radius combined with large discharge port size resulted to maximize the scroll  
11 efficiency. As regards the number of wraps, it should be chosen so as to avoid under-compression operating  
12 condition for the scroll. Minor effects have been reported as a consequence of the variation of the spiral  
13 thickness  
14

15 So, depending on the technical and/or economical constraints, such as mass flow rate, pressure ratio, size  
16 limits or motor characteristics (synchronous or asynchronous, with or without inverter, etc.), the optimal  
17 design is the best compromise between the above mentioned design guide-lines.  
18

19 A separate optimization has been carried out on the shape of the discharge port, showing a not-circular shape  
20 is more suitable for the compression dynamics.  
21

22 The high efficiency area found in the current work has two positive aspects. The first one is related to the  
23 flatness of the response surface close to the BEP. Such feature is always beneficial from the design  
24 standpoint, meaning that the machine is able to accommodate other types of constraints (e.g. the size of the  
25 discharge port) within a relatively large range. The second one is the fact that this area is also the one that is  
26 less sensitive to small input variations in terms of manufacturing imprecision.  
27

28  
29  
30 Finer optimization could be done considering different central geometries (asymmetrical scrolls and other  
31 different geometry correction at the central ends of the scrolls) as well as more complex 3D modifications  
32 (such as sweep extrusion instead of straight extrusion of the scroll profiles).  
33  
34  
35

## 36 **Acknowledgement**

37  
38  
39 This work was supported by the European Social Funds of Veneto Region (No. 2105-12-11-2018)  
40  
41  
42

## 43 **References**

- 44  
45  
46 [1] P. Song, M. Wei, L. Shi, S. N. Danish e C. Ma, «A review of scroll expanders for organic Rankine cycle  
47 systems,» *Applied Thermal Engineering*, vol. 75, p. 54–64, 2015.  
48  
49 [2] V. Lemort, S. Quoilin, C. Cuevas e J. Lebrun, «Testing and modeling a scroll expander integrated into  
50 an Organic Rankine Cycle,» *Applied Thermal Engineering*, vol. 29, p. 3094–3102, 2009.  
51  
52 [3] V. Lemort, S. Declaye e S. Quoilin, «Experimental characterization of a hermetic scroll expander for  
53 use in a micro-scale Rankine cycle,» *Proceedings of the Institution of Mechanical Engineers, Part A:  
54 Journal of Power and Energy*, vol. 226, p. 126–136, 2012.  
55  
56 [4] S. Declaye, S. Quoilin, L. Guillaume e V. Lemort, «Experimental study on an open-drive scroll  
57 expander integrated into an ORC (Organic Rankine Cycle) system with R245fa as working fluid,»  
58 *Energy*, vol. 55, p. 173–183, 2013.  
59  
60  
61  
62  
63  
64  
65

- 1  
2  
3  
4  
5  
6  
7  
8  
9  
10  
11  
12  
13  
14  
15  
16  
17  
18  
19  
20  
21  
22  
23  
24  
25  
26  
27  
28  
29  
30  
31  
32  
33  
34  
35  
36  
37  
38  
39  
40  
41  
42  
43  
44  
45  
46  
47  
48  
49  
50  
51  
52  
53  
54  
55  
56  
57  
58  
59  
60  
61  
62  
63  
64  
65
- [5] M. Morini, C. Pavan, M. Pinelli, E. Romito e A. Suman, «Analysis of a scroll machine for micro ORC applications by means of a RE/CFD methodology,» *Applied Thermal Engineering*, vol. 80, p. 132–140, 2015.
  - [6] A. Suman, S. Randi, N. Casari, M. Pinelli e L. Nespoli, «Experimental and numerical characterization of an oil-free scroll expander,» *Energy Procedia*, vol. 129, p. 403–410, 2017.
  - [7] X. Wang, Y. Hwang e R. Radermacher, «Two-stage heat pump system with vapor-injected scroll compressor using R410A as a refrigerant,» *International Journal of Refrigeration*, vol. 32, p. 1442–1451, 2009.
  - [8] M. Fukuta, T. Yanagisawa, O. Kosuda e Y. Ogi, «Performance of scroll expander for CO<sub>2</sub> refrigeration cycle,» 2006.
  - [9] D. Ziviani, M. Venturini e A. Beyene, «Advances and challenges in ORC systems modeling for low grade thermal energy recovery,» *Applied Energy*, vol. 121, p. 79–95, 2014.
  - [10] Y.-R. Lee e W.-F. Wu, «On the profile design of a scroll compressor,» *International journal of refrigeration*, vol. 18, p. 308–317, 1995.
  - [11] J. Wang, Q. Liu, C. Cao, Z. Wang, L. Qiang e Y. Qu, «Design methodology and geometric modeling of complete meshing profiles for scroll compressors,» *International Journal of Refrigeration*, vol. 91, p. 199–210, 2018.
  - [12] I. H. Bell, E. A. Groll, J. E. Braun, G. B. King e W. T. Horton, «Optimization of a scroll compressor for liquid flooding,» *International Journal of Refrigeration*, vol. 35, p. 1901–1913, 2012.
  - [13] C. Vessaz, L. Andolfatto, A. François e C. Tournier, «Toward design optimization of a Pelton turbine runner,» *Struct Multidisc Optimization*, vol. 55, pp. 37-51, 2017.
  - [14] A. Rossetti, G. Pavesi, G. Cavazzini, A. Santolin e G. Ardizzon, «Influence of the bucket geometry on the Pelton performance,» *Proceedings of the Institution of Mechanical Engineers, Part A: Journal of Power and Energy*, vol. 228, pp. 33-45, 2014.
  - [15] G. Cavazzini, G. Pavesi, A. Santolin, G. Ardizzon e R. Lorenzi, «Using splitter blades to improve suction performance of centrifugal impeller pumps,» *Proceedings of the Institution of Mechanical Engineers, Part A: Journal of Power and Energy*, vol. 229, pp. 309-323, 2015.
  - [16] N. Casari, A. Suman, M. Morini e M. Pinelli, «Real Gas Expansion with Dynamic Mesh in Common Positive Displacement Machines,» *Energy Procedia*, vol. 129, p. 248–255, 2017.
  - [17] N. Casari, A. Suman, D. Ziviani, M. Van Den Broek, M. De Paepe e M. Pinelli, «Computational Models for the Analysis of positive displacement machines: Real Gas and Dynamic Mesh,» *Energy Procedia*, vol. 129, p. 411–418, 2017.
  - [18] K.-Y. Kim, A. Samad e E. Benini, *Design optimization of fluid machinery*, Wiley, 2015.
  - [19] G. Ardizzon, G. Cavazzini e G. Pavesi, «Adaptive acceleration coefficients for a new search diversification strategy in particle swarm optimization algorithms,» *Information Sciences*, vol. 299, p. 337–378, 2015.
  - [20] H. Gao, H. Ding e Y. Jiang, «3D transient CFD simulation of scroll compressors with the tip seal,» *Materials Science and Engineering*, vol. 90, 2015.

- 1  
2  
3  
4  
5  
6  
7  
8  
9  
10  
11  
12  
13  
14  
15  
16  
17  
18  
19  
20  
21  
22  
23  
24  
25  
26  
27  
28  
29  
30  
31  
32  
33  
34  
35  
36  
37  
38  
39  
40  
41  
42  
43  
44  
45  
46  
47  
48  
49  
50  
51  
52  
53  
54  
55  
56  
57  
58  
59  
60  
61  
62  
63  
64  
65
- [21] A. Kovacevic, N. Stosic e I. Smith, «Screw compressors: three dimensional computational fluid dynamics and solid fluid interaction,» *Springer Science & Business Media.*, vol. 46, 2007.
- [22] J. Mandur e H. Budman, «Robust optimization of chemical processes using Bayesian description of parametric uncertainty,» *Journal of Process Control*, vol. 24, p. 422–430, 2014.
- [23] L. R. Ray e R. F. Stengel, «A Monte Carlo approach to the analysis of control system robustness,» *Automatica*, vol. 29, p. 229–236, 1993.
- [24] T. Ghisu, G. T. Parks, J. P. Jarrett e P. J. Clarkson, «Robust design optimization of gas turbine compression systems,» *Journal of Propulsion and power*, vol. 27, p. 282–295, 2011.
- [25] D. Ziviani, A. Suman, S. Lecompte, M. De Paepe, M. van den Broek, P. R. Spina, M. Pinelli, M. Venturini e A. Beyene, «Comparison of a single-screw and a scroll expander under part-load conditions for low-grade heat recovery ORC systems,» *Energy Procedia*, vol. 61, p. 117–120, 2014.
- [26] D. Del Campo, R. Castilla, G. A. Raush, P. G. Montero e E. Codina, «Numerical analysis of external gear pumps including cavitation,» *Journal of fluids engineering*, vol. 134, p. 081105, 2012.